# Autonomous screening for Diabetic Macular Edema using deep learning processing of retinal images

Idan Bressler [1], Rachelle Aviv [1], Danny Margalit [1], Sean Ianchulev [1, 2], Zack Dvey-Aharon [1]

[1] AEYE Health Inc

[2] New York Eye and Ear, Mount Sinai Hospital, NY

## Abstract

**Background:** Diabetic Macular Edema (DME) is a complication of diabetes which, when untreated, leads to vision loss. Screening for DME is recommended for diabetic patients every 1-2 years, however compliance rates are low. Though there is currently no high-efficacy camera-agnostic system for DME detection, an AI system may improve compliance.

**Methods:** A deep learning model was trained for DME detection using the EyePacs dataset. Data was randomly assigned, by participant, into development (n= 14,246) and validation (n= 1,583) sets. Analysis was conducted at the single image, eye, and patient levels. Model performance was evaluated using sensitivity, specificity, and AUC.

**Findings:** At the patient level, sensitivity of 0.901 (CI 95% 0.879-0.917), specificity of 0.900 (CI 95% 0.883-0.911), and AUC of 0.962 (CI 95% 0.955-0.968) were achieved. At the image level, sensitivity of 0.889 (CI 95% 0.878-0.900), specificity of 0.889 (CI 95% 0.877-0.900), and AUC of 0.954 (CI 95% 0.949-0.959) were achieved. At the eye level, sensitivity of 0.905 (CI 95% 0.890-0.920), specificity of 0.902 (CI 95% 0.890-0.913), and AUC of 0.964 (CI 95% 0.958-0.969) were achieved.

**Interpretation:** DME can be detected from color fundus imaging with high performance on all analysis metrics. Automatic DME detection may simplify screening, leading to more comprehensive screening for diabetic patients. Further prospective studies are necessary.

**Funding:** Provided by AEYE Health Inc.

## Introduction

Diabetic Macular Edema (DME) is a complication of diabetes mellitus, closely associated with Diabetic Retinopathy (DR)[1]. DME is characterized by the accumulation of excess fluid in the extracellular space within the central macula[2,3], and when untreated ultimately leads to vision loss due to photoreceptor damage of the fovea, which is responsible for high resolution visual acuity. DME has a major impact on the health of the general population as it affects approximately 3.8% of the population[4], with an incidence rate of over 25% within 25 years of diagnosis of type 1 diabetes mellitus (T1DM)[5] and over 25% within 9 years of type 2 diabetes mellitus (T2DM) diagnosis[6].

The Early Treatment Diabetic Retinopathy Study (ETDRS) defined clinically significant DME (CSME) using specific anatomic criteria which include retinal thickening or existence of hard exudates in the foveal area (500 μm around the fovea)[7]. Additionally, the ETDRS set forth a treatment protocol treatment which now includes focal laser photocoagulation, intravitreal anti-vascular endothelial growth factor (anti-VEGF) therapy and other emerging treatments, which have shown significant improvement in prognosis and visual acuity restoration after treatment[8–10]. Therefore, detection, and specifically early detection, is crucial in improving patient outcomes.

Screening for DME is conducted as a part of regular screening and management for diabetic retinopathy (DR), and typically involves slit lamp examination or fundus photography[11]. Screening for DR and DME is recommended for diabetic patients every 1-2 years[11,12]. While conventional diagnosis of CSME/DME has been based on fundus photography and fluorescein angiography, more recently Optical Coherence Tomography (OCT) has been increasingly used to detect diabetes-related typical retinal thickening [13,14]. However, this expensive modality is mostly available at specialized eye clinics and not generally accessible for primary and widespread screening purposes. Diagnosis of CSME/DME is also done using color fundus imaging, based on patterns of DME which match the aforementioned criteria for CSME, and specifically exudates and macular deformations[10,15,16].

Access and scalability are crucial to any population health screening program. The need for a specialized eye examination and sophisticated equipment have presented significant obstacles to streamlined DME screening and many patients go undiagnosed[17–20]. Machine learning and deep learning algorithms are ideal tools to address this limitation and empower an efficient and exponential screening process, at the level of primary non-specialized care delivery.

Methods for DR screening using deep learning algorithms which examine fundus imaging have shown promising results[21,22]. Furthermore, autonomous DR screening has achieved FDA approval[23,24], showing a high potential for the implementation of further similar applications, such as DME screening.

OCT-based machine learning methods have shown good results in DME detection[25–27], with some methods boasting almost 100% accuracy. Unfortunately, as stated, OCT is far less accessible than fundus photography, and thus less suited for screening purposes.

Other methods using fundus imagery and focusing on exudate detection were previously developed[28–32], as well as methods based on the entire CSME criteria[33,34]. The method presented in this paper improves DME detection efficacy compared to previous works, while complying with the full CSME definition. Additionally, this work expands analysis from the single image level to the eye and patient level, which have better clinical relevance.

## Methods

### Data

The main dataset utilized for training and validation was compiled and provided by EyePACs[35] and consisted of 45° angle fundus photography images and expert readings of said images. All images and data were de-identified according to the Health Insurance Portability and Accountability Act “Safe Harbor” before they were transferred to the researchers. Institutional Review Board exemption was obtained.

A comprehensive dataset sampled from the EyePACs dataset , Two images were taken for each eye from two different fields, one centered on the macula and another centered between the macula and the disc. The average age of patients was 55.02 (10.21 S.D), 51% of the patients were female (**Table 1**).

Each eye underwent expert reading, including but not limited to DME presence, DR level, and image quality. It should be noted that image quality assessment was based on the overall readability, meaning the ability to provide a DR/DME reading, of a given eye and does not guarantee that all images of said eye are of the same quality. All images labeled as readable by an expert were used, resulting in 32,049 images from 15,892 patients. **Table 2** shows the distribution of DME patients across DR levels; DME is only present for patients with more than mild DR, with approximately 49% of all images being DME positive. Additional statistics are provided in **supplementary tables 1-2**.

A secondary dataset used for validation was the Messidor-2 dataset[36], also containing 45° angle fundus photography images and expert annotations for DME presence and DR level. The dataset consisted of 1748 macula centered images from 874 examinations, of which 151 images (8.6%) were DME positive. Additional information is provided in **supplementary table 3**.

### Pre-Processing

Image pre-processing was performed in two steps. Firstly the image background was cut along the convex hull which contains the circular border between the image and the background. **Figure 1** shows a sample result of this process. Secondly, images were resized to 512X512 pixels.

### Quality assessment

A tool for image quality assessment was developed based on detecting visibility of fundus specific characteristics. The given quality score for an image was an aggregation of the visibility score from multiple areas within the fundus image. **Figure 2** demonstrates a few examples of

images and their respective scores, showing the correlation between score and visual image quality.

### Model training

The data was divided into training, validation, and test datasets consisting of 80%, 10%, and 10% of the data respectively.

A binary classification neural network was trained. The model architecture was automatically fitted to best balance the model performance vs model complexity tradeoff. Hyperparameter tuning was done over the validation set.

Using the aforementioned quality assessment tool, low quality images were filtered out before training. The image quality threshold was set at the point at which model performances stopped improving by filtering additional images, resulting in 1,978 images filtered (approximately 6.2% of the data).

### Statistical analysis

The metrics used for assessment were accuracy, sensitivity, specificity, and area under the receiver operating characteristic curve (AUC). For each metric the bias corrected and accelerated bootstrap method[37] was used to produce a 95% confidence interval.

### Analysis levels

DME detection was performed on three different levels. The first, namely detection at the individual image level, was the basic task for which the model was trained. The second level was detection at the eye level using both fields from a given eye, following the way DME is detected by a human expert. In this approach, the best image for each eye (in terms of image quality as assessed by the image quality tool) was selected for analysis. The third level was the patient level. For clinical purposes, detection of DME in one eye is sufficient for referral to further checks. Therefore, in this approach the results from both eyes were compared and the eye with the higher model probability was selected to produce a patient level result.

## Results

### EyePACs dataset

The results for the different analysis methods were as follows (**table 3**): For the image level, sensitivity of 0.889 (CI 95% 0.878, 0.900) and specificity of 0.889 (CI 95% 0.877, 0.900) was achieved. For the eye level, sensitivity of 0.905 (CI 95% 0.890, 0.920) and specificity of 0.902 (CI 95%0.890, 0.913) was achieved. For the patient level, sensitivity of 0.901 (CI 95% 0.879, 0.917) and specificity of 0.900 (CI 95% 0.883, 0.911) was achieved.

The results for each DR level for which DME is present are displayed in **table 4**, showing comparable results across all DR levels. The model archived 0.958 (CI 95% 0.952, 0.964) AUC for DR level 2, 0.935 (CI 95% 0.923, 0.945) AUC for DR level 3, 0.940 (CI 95% 0.926, 0.952) AUC for DR level 4 and 0.954 (CI 95% 0.919, 0.975) AUC for ungradable DR level. DR grades

0 and 1 did not have any DME positive examples; thus most metrics are not defined; the model achieved 0.981 (CI not defined) and 0.876 accuracy for grades 0 and 1 respectively.

**Table 5** shows the results for images which passed (high quality) and did not pass (low quality) the quality filter, showing significant differences between the populations. The results for images which were filtered out were 0.671 (CI 95% 0.599, 0.737) sensitivity, 0.843 (CI 95% 0.790, 0.886) specificity, and 0.853 (CI 95% 0.811, 0.887) AUC. Results for images which passed the quality filter were 0.902 (CI 95% 0.892, 0.912) sensitivity, 0.883 (CI 95% 0.871, 0.893) specificity and 0.956 (CI 95% 0.952, 0.961) AUC. The filter allowed for a reading at the patient level of 98% of the patient cohort.

### Messidor-2 dataset

Messidor-2 contained readings for the image and patient levels, containing one image per eye. The results on this data set were an AUC of 0.971 (CI 95% 0.955 - 0.982), 0.875 (CI 95% 0.811 - 0.922) sensitivity, and 0.954 (CI 95% 0.939 - 0.967) specificity, surpassing previous works (**table 6**). At the patient level an AUC of 0.964 (CI 95% 0.936, 0.979), sensitivity of 0.897, (CI 95% 0.820, 0.947) and specificity of 0.932 (CI 95% 0.905, 0.953) were achieved.

## Discussion

This work introduced a proprietary autonomous system for the detection of DME from fundus images, which may shorten and simplify screening processes and allow for wider screening of DME. Given the short (≤ 3 months) recommended referral time after DME detection[11], and potential threat to patients' vision if untreated, widespread autonomous screening has the potential to be of clinical importance.

The need to screen for DME independently from autonomous screening for DR stems from two main factors. Firstly, the recommended referral time for DME is shorter than for most DR cases without DME[11]. Secondly the treatment regime for DME differs from the treatment for DR without DME[38], emphasizing the importance of distinguishing DME cases from DR cases.

This work proposed analyzing DME on multiple levels, expanding on existing works which focused on the single image level. On the image level, this method shows higher efficacy compared to previous studies. Additionally, it showed comparable results between the Messidor-2 dataset and the less curated (in terms of image quality) EyePACs dataset, demonstrating its robustness across different image qualities. The model is capable of producing a reading for the vast majority of examined patients, further supporting the possible widespread capabilities and applications. Analysis at the eye level, using multiple images of the same eye, may be more accurate and representative of clinical practice than image level analysis. When multiple fields of the same eye exist, experts label images based on the integration of present information. This may lead to the labeling of individual images being misleading, especially if differences in image quality exist. For instance, an eye that appears

healthy from one angle, often due to low image quality, might have DME in another, leading to a seemingly healthy image being positively labeled. The presented eye-level analysis tackles this issue by selecting the best field from each eye.

Analysis at the patient level may be the most clinically relevant, more than at the single image level or the eye level, as the overall clinical criterion for referral is the existence of DME at the patient level. This method combined the results from both eyes to produce a patient level result, demonstrating high (~90%) sensitivity and specificity.

CSME with foveal involvement is also known as CMSE with Center Involvement (CSME-CI)[2,11], and the ability of graders to consistently detect this has been questioned[39]. Detection of CSME remains common clinical practice and a referral marker. Despite CSME-CI being more severe than non CI CSME, all CSME cases are referable, thus making widespread screening of CSME important. This paper therefore focuses on CSME detection and not CSME-CI detection.

The presence of hard exudates within one disc diameter of the macula has been used in many works for automatic detection of DME. More specifically, Gulshan et al. showed comparable results when using deep learning for DME detection according to this definition[28]. However, this definition does not comply with the full CSME definition and thus does not cover all of the cases, and the best method of exudate based DME analysis is up for debate[40]. Litvin Et al[41] shows that using exclusively hard exudates, in comparison to the entire CSME of exudates and swelling, does not yield the same gradings, meaning that there are relevant cases which are missed by this method. Our work presents comparable results using a wider definition of CSME and a more comprehensive screening tool.

This work has several limitations. Firstly, model training was still done at the single image level, thus hindering the training with the aforementioned problem with image labeling. Secondly, this work lacks prospective clinical experiments to validate the results.

## Figures and tables

| Field | Images | Patients | Mean Age (s.d) | Gender (% Female) | Ethnicity (fraction) |
|---|---|---|---|---|---|
| Value | 32,049 | 15,892 | 55.02 (10.21) | 51 | White = 0.55 (Hispanic = 0.93, non Hispanic = 0.07)<br>ethnicity not specified = 0.13<br>African descent = 0.11<br>Indian subcontinent origin = 0.10<br>Asian = 0.03<br>Other = 0.08 |

**Table 1**. Patient numbers and population statistics for the EyePACs dataset

| DR grade | 0 | 1 | 2 | 3 | 4 | Ungradable |
|---|---|---|---|---|---|---|
| Image count | 1,461 | 116 | 16,707 | 7,806 | 5,051 | 908 |
| DME | 0 | 0 | 8,405 | 4,060 | 2,632 | 498 |
| No DME | 1,461 | 116 | 8,302 | 3,746 | 2,419 | 410 |

**Table 2**. Patient numbers and DME prevalence across DR grades for the EyePACs dataset.

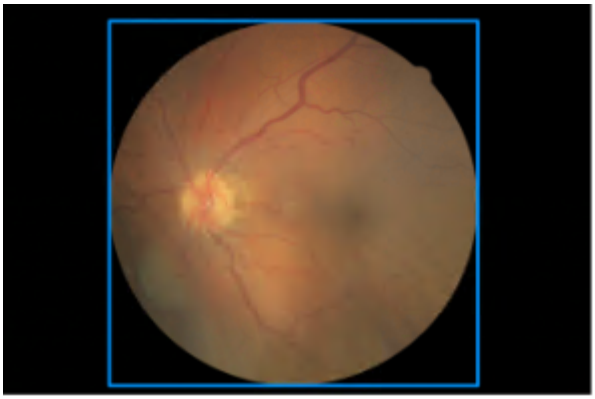

**Figure 1**. Example of image cropping, blue line represents the cropping boundaries


**Figure 2**. Example images and their accompanying image quality scores, ordered from worst quality (left) to best quality (right)

| | Accuracy(C.I) | Sensitivity(C.I) | Specificity(C.I) | AUC(C.I) |
|---|---|---|---|---|
| Image level | 0.889 (0.881, 0.897) | 0.889 (0.878, 0.900) | 0.889 (0.877, 0.900) | 0.954 (0.949, 0.959) |
| Eye Level | 0.903 (0.894, 0.912) | 0.905 (0.890, 0.920) | 0.902 (0.890, 0.913) | 0.964 (0.958, 0.969) |
| Patient level | 0.898 (0.886, 0.909) | 0.900 (0.879, 0.917) | 0.900 (0.883, 0.911) | 0.962 (0.955, 0.968) |

**Table 3**. Results for the EyePACs dataset across all three analysis levels, given in accuracy, sensitivity, specificity and AUC with a 95% confidence interval.

| DR grade | 2 | 3 | 4 | Ungradable |
|---|---|---|---|---|
| Sensitivity (C.I) | 0.908 (0.893, 0.921) | 0.900 (0.877, 0.918) | 0.899 (0.875, 0.921) | 0.860 (0.784, 0.917) |
| Specificity (C.I) | 0.897 (0.881, 0.911) | 0.826 (0.798, 0.880) | 0.863 (0.828, 0.893) | 0.920 (0.811, 0.978) |
| AUC (C.I) | 0.962 (0.956, 0.968) | 0.939 (0.928, 0.949) | 0.943 (0.928, 0.955) | 0.961 (0.926, 0.981) |

**Table 4**. Results for the EyePACs dataset across DR grades, given in accuracy, sensitivity, specificity and AUC with a 95% confidence interval.

| | Sensitivity(C.I) | Specificity(C.I) | AUC(C.I) |
|---|---|---|---|
| Filtered out | 0.69 (0.611, 0.761) | 0.858 (0.805, 0.900) | 0.862 (0.819, 0.897) |
| Remained | 0.890 (0.879, 0.901) | 0.883 (0.871, 0.894) | 0.952 (0.948, 0.957) |

**Table 5**. Results for images filtered out and not filtered out by the image quality tool, given in accuracy, sensitivity, specificity and AUC with a 95% confidence interval.

| | Accuracy(C.I) | Sensitivity(C.I) | Specificity(C.I) | AUC(C.I) |
|---|---|---|---|---|
| Sahlsten et al [33] | 0.931 (0.915, 0.944) | 0.69 (0.626, 0.750) | 0.989 (0.980, 0.994) | 0.932 (0.917, 0.946) |
| Li et al [34] | - | 0.886 (0.881, 0.892) | 0.908 (0.898, 0.912) | 0.948 (0.943, 0.951) |
| Proposed, image level | 0.943 (0.927, 0.955) | 0.875 (0.811, 0.922) | 0.954 (0.939, 0.967) | 0.971 (0.955, 0.982) |
| Proposed, patient level | 0.925 (0.898, 0.944) | 0.897 (0.820, 0.947) | 0.932 (0.905, 0.953) | 0.964 (0.936, 0.979) |

**Table 6**, Comparison between the proposed method and previous works on the Messidor-2 dataset, given in accuracy, sensitivity, specificity and AUC with a 95% confidence interval. Additionally results on the patient level (not performed in previous works) are given.

## Bibliography

1 Mohamed Q, Gillies MC, Wong TY. Management of diabetic retinopathy: a systematic review. *JAMA* 2007; **298**: 902–16.

2 Lang GE. Diabetic Macular Edema. *OPH* 2012; **227**: 21–9.

3 Bandello F, Parodi MB, Lanzetta P, *et al.* Diabetic Macular Edema. In: Macular Edema. Karger Publishers, 2010: 73–110.

4 Varma R, Bressler NM, Doan QV, *et al.* Prevalence of and risk factors for diabetic macular edema in the United States. *JAMA Ophthalmol* 2014; **132**: 1334–40.

5 Klein R, Klein BEK, Moss SE, Cruickshanks KJ. The Wisconsin epidemiologic study of diabetic retinopathy XV. *Ophthalmology* 1995; **102**: 7–16.

6 White NH, Sun W, Cleary PA, *et al.* Effect of prior intensive therapy in type 1 diabetes on 10-year progression of retinopathy in the DCCT/EDIC: comparison of adults and adolescents. *Diabetes* 2010; **59**: 1244–53.

7 Grading diabetic retinopathy from stereoscopic color fundus photographs—an extension of the modified Airlie house classification. *Ophthalmology* 1991; **98**: 786–806.

8 Diabetic Retinopathy Clinical Research Network, Elman MJ, Aiello LP, *et al.* Randomized trial evaluating ranibizumab plus prompt or deferred laser or triamcinolone plus prompt laser for diabetic macular edema. *Ophthalmology* 2010; **117**: 1064-1077.e35.

9 Kim EJ, Lin WV, Rodriguez SM, Chen A, Loya A, Weng CY. Treatment of Diabetic Macular Edema. *Curr Diab Rep* 2019; **19**: 68.

10 Bhagat N, Grigorian RA, Tutela A, Zarbin MA. Diabetic macular edema: pathogenesis and treatment. *Surv Ophthalmol* 2009; **54**: 1–32.

11 International Diabetes Federation. Clinical Practice Recommendations for Managing Diabetic Macular Edema. Brussels, Belgium: International Diabetes Federation, 2019 https://www.idf.org/e-library/guidelines/161-dme-clinical-practice-recommendations.html.

12 American Diabetes Association Professional Practice Committee, Draznin B, Aroda VR, *et al.* Retinopathy, Neuropathy, and Foot Care: Standards of Medical Care in Diabetes-2022. *Diabetes Care* 2022; **45**: S185–94.

13 Panozzo G, Parolini B, Gusson E, *et al.* Diabetic macular edema: an OCT-based classification. *Semin Ophthalmol* 2004; **19**: 13–20.

14 Panozzo G, Gusson E, Parolini B, Mercanti A. Role of OCT in the diagnosis and follow up of diabetic macular edema. *Semin Ophthalmol* 2003; **18**: 74–81.

15 Bresnick GH. Diabetic macular edema. A review. *Ophthalmology* 1986; **93**: 989–97.

16 Vujosevic S, Casciano M, Pilotto E, Boccassini B, Varano M, Midena E. Diabetic macular edema: fundus autofluorescence and functional correlations. *Invest Ophthalmol Vis Sci* 2011; **52**: 442–8.

17 Garg S, Davis RM. Diabetic retinopathy screening update. *Clin Diabetes* 2009; **27**: 140–5.

18 Lewis K. Improving patient compliance with diabetic retinopathy screening and treatment. *Community Eye Health* 2015; **28**: 68–9.

19 Kiire CA, Porta M, Chong V. Medical management for the prevention and treatment of diabetic macular edema. *Surv Ophthalmol* 2013; **58**: 459–65.

20 Saadine JB, Fong DS, Yao J. Factors associated with follow-up eye examinations among persons with diabetes. *Retina Phila Pa* 2008; **28**: 195–200.

21 Alyoubi WL, Shalash WM, Abulkhair MF. Diabetic retinopathy detection through deep learning techniques: A review. *Inf Med Unlocked* 2020; **20**: 100377.

22 Grzybowski A, Brona P, Lim G, *et al.* Artificial intelligence for diabetic retinopathy screening: a review. *Eye* 2020; **34**: 451–60.

23 Abràmoff MD, Lavin PT, Birch M, Shah N, Folk JC. Pivotal trial of an autonomous AI-based diagnostic system for detection of diabetic retinopathy in primary care offices. *Npj Digit Med* 2018; **1**: 1–8.

24 Raman R, Srinivasan S, Virmani S, Sivaprasad S, Rao C, Rajalakshmi R. Fundus photograph-based deep learning algorithms in detecting diabetic retinopathy. *Eye* 2019; **33**: 97–109.

25 Alsaih K, Lemaitre G, Rastgoo M, Massich J, Sidibé D, Meriaudeau F. Machine learning techniques for diabetic macular edema (DME) classification on SD-OCT images. *Biomed Eng Online* 2017; **16**: 68.

26 Kaymak S, Serener A. Automated age-related macular degeneration and diabetic macular edema detection on OCT images using deep learning. IEEE, 2018. DOI:10.1109/iccp.2018.8516635.

27 Kermany DS, Goldbaum M, Cai W, *et al.* Identifying Medical Diagnoses and Treatable Diseases by Image-Based Deep Learning. *Cell* 2018; **172**: 1122-1131.e9.

28 Gulshan V, Peng L, Coram M, *et al.* Development and Validation of a Deep Learning Algorithm for Detection of Diabetic Retinopathy in Retinal Fundus Photographs. *JAMA* 2016; **316**: 2402–10.

29 Mo J, Zhang L, Feng Y. Exudate-based diabetic macular edema recognition in retinal images using cascaded deep residual networks. *Neurocomputing* 2018; **290**: 161–71.

30 Perdomo O, Otalora S, Rodríguez F, Arevalo J, González FA. A novel machine learning model based on exudate localization to detect diabetic macular edema. In: Proceedings of the Ophthalmic Medical Image Analysis Third International Workshop. Iowa City, IA: University of Iowa, 2016.

31 Giancardo L, Meriaudeau F, Karnowski TP, *et al.* Exudate-based diabetic macular edema detection in fundus images using publicly available datasets. *Med Image Anal* 2012; **16**: 216–26.

32 Lim ST, Zaki WMDW, Hussain A, Lim SL, Kusalavan S. Automatic classification of diabetic macular edema in digital fundus images. IEEE, 2011. DOI:10.1109/chuser.2011.6163730.

33 Sahlsten J, Jaskari J, Kivinen J, *et al.* Deep Learning Fundus Image Analysis for Diabetic Retinopathy and Macular Edema Grading. *Sci Rep* 2019; **9**: 10750.

34 Li F, Wang Y, Xu T, *et al.* Deep learning-based automated detection for diabetic retinopathy and diabetic macular oedema in retinal fundus photographs. *Eye* 2021; published online July 1. DOI:10.1038/s41433-021-01552-8.

35 Diabetic Retinopathy Screening. EyePACS. 2018; published online Nov. https://www.eyepacs.com/.

36 Decencière E, Zhang X, Cazuguel G, *et al.* Feedback on a publicly distributed image database: The Messidor database. *Image Anal Ster* 2014; **33**: 231.

37 Efron B, Tibshirani RJ. An introduction to the bootstrap: CRC press. *Ekman P Friesen WV 1978 Man Facial Action Coding Syst* 1994.

38 Mansour SE, Browning DJ, Wong K, Flynn HW Jr, Bhavsar AR. The Evolving Treatment of Diabetic Retinopathy. *Clin Ophthalmol* 2020; **14**: 653–78.

39 Date RC, Shen KL, Shah BM, Sigalos-Rivera MA, Chu YI, Weng CY. Accuracy of Detection and Grading of Diabetic Retinopathy and Diabetic Macular Edema Using Teleretinal Screening. *Ophthalmol Retina* 2019; **3**: 343–9.

40 Litvin TV, Bresnick GH, Cuadros JA, Selvin S, Kanai K, Ozawa GY. A Revised Approach for the Detection of Sight-Threatening Diabetic Macular Edema. *JAMA Ophthalmol* 2017; **135**: 62–8.

41 Litvin TV, Ozawa GY, Bresnick GH, *et al.* Utility of hard exudates for the screening of macular edema. *Optom Vis Sci* 2014; **91**: 370–5.